DOI: http://dx.doi.org/10.18524/1810-4215.2016.29.85048

3D NUMERICAL HYDRODYNAMICAL SIMULATIONS OF A RADIATION-DRIVEN JET LAUNCH AND DISAPPEARING OVER LOW/HARD STATE

V.V. Nazarenko, S.V. Nazarenko

Astronomical Observatory, Odessa National University,
Shevchenko Park, Odessa, 65014, Ukraine, *nazaret@te.net.ua*

ABSTRACT. In the present research we have calculated 3D numerical hydrodynamical simulations of a radiation-driven jet launch and disappearing over low/hard state. The calculations show that the jet launch occurs at the beginning of the low/hard state over 10-30 minutes of the orbital time. The jet disappearing occurs over the short time scale (of the order of 10-30 minutes of the orbital time) at the end of the low/hard state. The calculations also show that the temperature near the accretor is increased in 100-200 times over low/hard state relatively high/soft. The mass accretion rate in the disc is anti-correlated with the temperature near the accretor in our calculations.

Keywords: Stars: binaries - stars: jets - methods: numerical - hydrodynamics.

1. Introduction

The present research is concerned the 3D numerical hydrodynamical simulations of a radiation-driven jet launch and disappearing over low/hard states in microquasar on the base of Cyg X-1 binary parameters. The microquasars are that in semi-detached close binary systems in which the normal star (supergiant of O-B classes) overfill its Roche lobe and inflowing via L_1-stream in the compact objects (neutron star or black hole) Roche lobe in which accretion disc around the accretor is formed. Microquasar phenomenon is a launch and disappearing of relativistic jet along disc rotation access in low/hard and high/soft states respectively. The observations show that jet velocities are about values: 0.25 and 0.98–0.99 of light speed. The observations also show that accretion disc luminosities in microquasars are about of 0.1–0.5 of critical luminosity (Fender et al., 1999; Fender, 2001; Mirabel, 2001; Fender, Gallo , Jonker, 2003; Fender, Belloni, Gallo, 2004; Gallo & Fender, 2005; Fender et al., 2006; Lachowicz et al., 2006; Gallo, 2007). The present work is the third one of own works which are devoted to 3D numerical hydrodynamical simulations of microquasar phenomenon. We have simulated low/hard and high/soft states in accretion disc of microquasar Cyg X-1 taking into account the constant precession in the first work (Nazarenko V. & Nazarenko S., 2014) and undefined precession in the second one (Nazarenko V. & Nazarenko S., 2015). These results show the disc central part temperature is increased in 100–200 times over low/hard state relatively the central disc part temperature in high/soft state. The disc mass accretion rate is anti-correlated relatively the central disc part temperature time behaviour. The mass accretion rate is decreasing in 50–100 times over low/hard state relatively high/soft. The central disc part temperature is maximal at the beginning and at the end of the low/hard state. The transition between both states described above is order of 10–30 minutes of the orbital time. This time interval is very small value in respect to with the duration of both states described above since that of these states are about of half of the precession period (7–8 days in our calculations). In the first work (Nazarenko V. & Nazarenko S., 2014) the transitions between both states are regularly and happen every precession period. In the second work (Nazarenko V. & Nazarenko S., 2015) the transitions between both states are irregularly and are not every precession period. Such the numerical properties of the microquasar phenomenon calculated by us are close to the observational properties of classical microquasar Cyg X-1.

In the present work we complicate our simulations of microquasar phenomenon. For that we will calculate the radiation-driven jet formation along the disc rotation access simultaneously with the simulation of low/hard and high/soft states in an accretion disc of classical microquasar Cyg X-1. Thus, our main task is to calculate the radiation-driven jet formation and its time behaviour over low/hard and high/soft states in classical microquasar Cyg X-1.

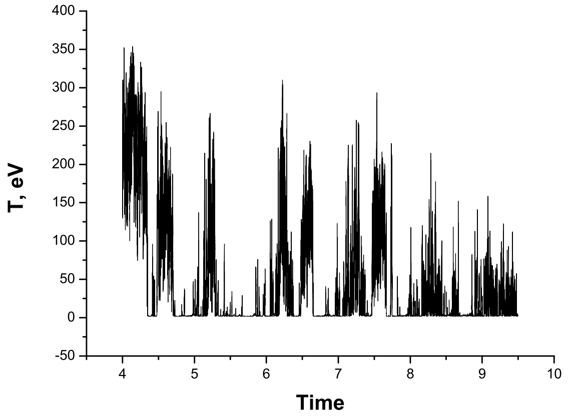

Figure 1: The time-dependences of the disc central part temperature.

2. Numerical algorithm

In the present research we use the numerical algorithm that is identical to our previous works. Shortly, the algorithm consists in the following. To calculate the accretion disc, we compute mass flow in the calculation area from initial to steady state. For that we use non-stationary hydrodynamical Euler equations which are resolved by astrophysical variant of the big particle code by Belotserkovskii & Davydov (1982). In the present research we use the radiation cooling model accordingly to Cox D.P. & Daltabuit E. (1971). To calculate mass flow in the calculation area we use rectangular coordinate system and numerical greed. The sell number in the numerical greed is 110×110×148. To focus the jets along the disc rotation axes we will calculate the component of the radiation forces only. These radiation forces will be calculated by us in the approach of optically thin layers and in the approach of LTE and they may be written as follows: $F_{rad} = \alpha * H/c$, where α is a coefficient of Thompsons scattering; H is radiation flux written as $\sigma * T^4$; c is light speed. To simulate accretion disc precession we simulated slaved precession.

We use the following dimensionless units. The density is given in units of 10^{11} particles per cm^3; all the distances are given in units of the orbital separation; all temperatures are given in units of eV; the velocities are given in $km\ s^{-1}$.

We cut the space around accretor with the radius of 0.05 to avoid the singularity in our calculations. We name this volume as Accretor-1 to distinguishit from real accretor.

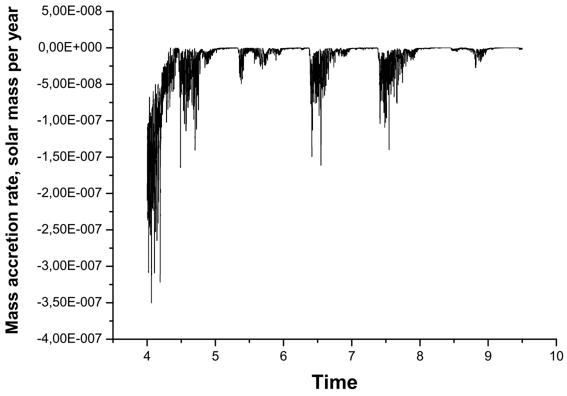

Figure 2: The time-dependences of the disc mass accretion rate.

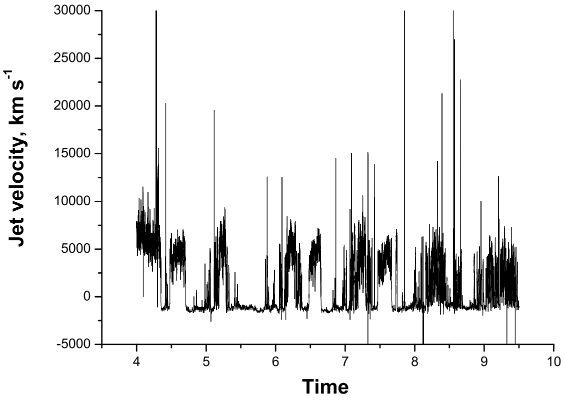

Figure 3: The time-dependences of the jet velocity.

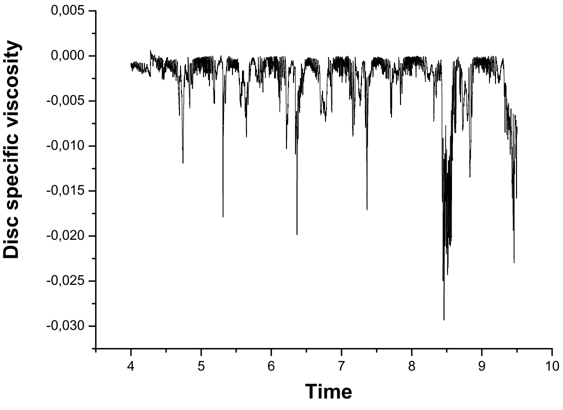

Figure 4: The time-dependences of the disc viscosity.

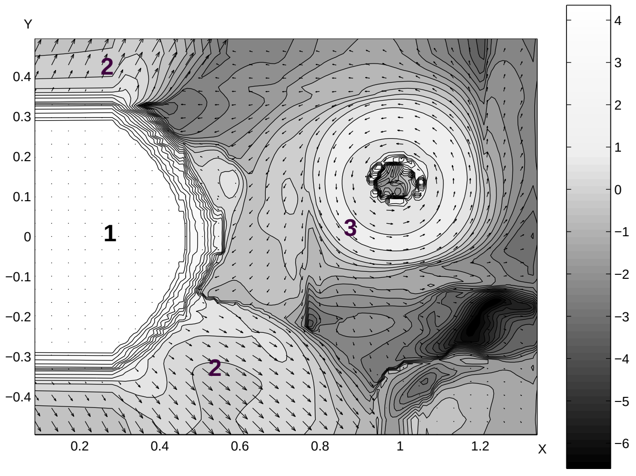

Figure 5: The cross-section of the calculation area by orbital plane and density contours on time 7.6 precession period.

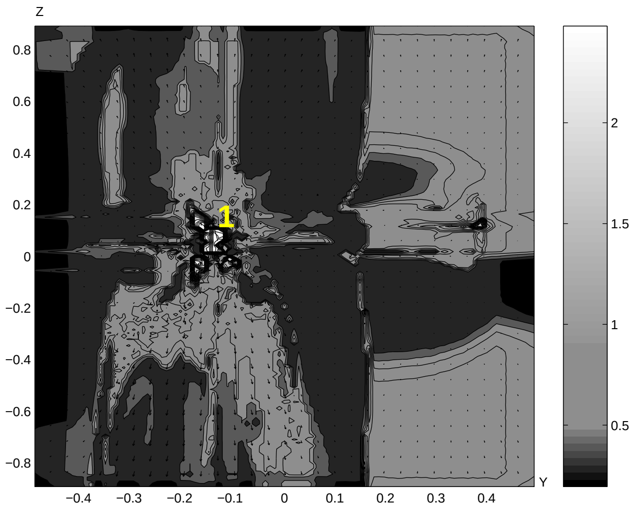

Figure 6: The cross-section of the calculation area by $Z-Y$ plane laying on compact object centre on low resolution space scale and temperature contours on time 7.6 precession period.

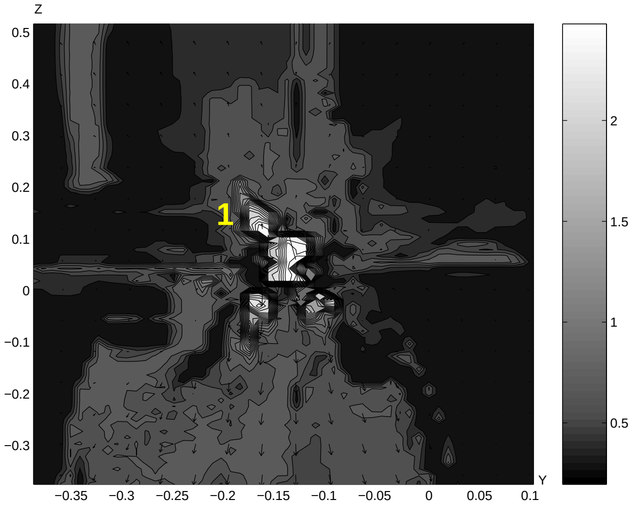

Figure 7: The cross-section of the calculation area by $Z-Y$ plane laying on compact object centre on high resolution space scale and temperature contours on time 7.6 precession period.

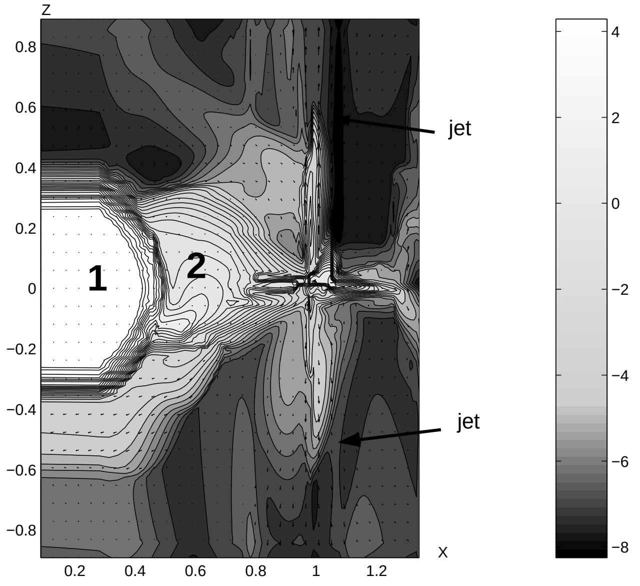

Figure 8: The cross-section of the calculation area by $Z-X$ plane laying on line of centres and density contours on time 7.6 precession period.

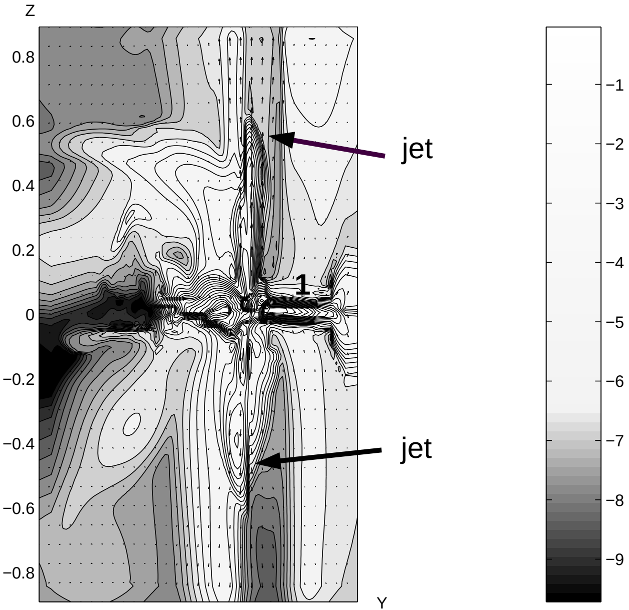

Figure 9: The cross-section of the calculation area by $Z-Y$ plane laying on compact object centre and temperature contours on time 7.6 precession period.

3. Results

In our present simulations one-armed jets will be simulated in essential. By this reason we will show the jet parameters upper Acretor-1 only along the disk rotation axis at a height as high as 0.04.

The main results of the present research are plotted in Fig. 1-4. The time behaviour of the disc central part temperature is plotted in Fig. 1; the disc mass accretion rate is plotted in Fig. 2; jet velocity is plotted in Fig. 3; the accretion disc viscosity plotted in Fig. 4 is calculated as $V_{rad} * r$, where V_{rad} is radial velocity given in units of the orbital speed and r is the radial coordinate given in units of the orbital separation. The Fig. 1 shows that the temperatures in the disc central part are into two states: high and low. In the high state the temperatures are more high than the temperatures in the low states in 100-200 times approximately. The Fig. 2 shows that the mass accretion rate is anti-correlated with Fig. 1. When the temperature is high in Fig. 1, mass accretion rate is decreasing in 50-100 times. The key parameters in the present research are the jet velocities calculated along the disc rotation axis at a height as high as 0.04 (see Fig. 3). If jets are launching, the jet velocity is positive and on contrary when jets are disappearing, the jet velocity is negative (see Fig. 3) and an accretion process on compact object occurs. As Fig. 3 shows, the jet launch in the present research occurs suddenly, over 10-30 minutes of the orbital time, and its disappearing is also occurring suddenly over the same time. Analysing the presenting Fig. 1-3 we may finally conclude that low/hard and high/soft states are simulated in our present research (Fender et al., 1999; Fender, 2001; Fender, Gallo, Jonker, 2003; Fender, Belloni, Gallo, 2004; Gallo & Fender, 2005; Fender et al., 2006). As Fig. 3 also shows, the jet velocities are maximal at the beginning and at the end of the low/hard state. This jet property may be explained very simply: the force accelerated jets is suddenly increased and is maximal at the beginning and the end of low/hard state but the jet mass is increased more gradually and is not maximal at the time pointed above. Such the circumstance finally results accordingly second Newtons law in the maximal jet velocity at the time stated above. The important parameter in the present research is an accretion disc specific viscosity. This parameter calculated in the present research (see Fig. 4) is maximal before a starting of jets. We may also mark that all the essential physical parameters of both states and jet production (see Fig. 1-4) are strong fluctuated over low/hard state in the present simulations.

The explanation of a mechanism of the jet production and low/hard and high/soft states generated in the present research is very simple: due to the precession of an accretion disc having being blowing by the donors wind in a disc in its central part to states are generated with high and low densities. When density is high in the disc centre and taking into account that optical thickness is less than 1 in this volume, the energy is very rapidly radiated due to radiation cooling and the temperature is very low in this state. On contrary, when the densities are low in the disc centre, the radiation cooling is not efficient in this volume and due to disc viscosity the kinetic energy of the disc rotation is instantaneously transformed into heat and the temperature is suddenly increased in this volume.

The cross-section of the calculation area by the disc plane (the density contours and velocity field; the precession phase is about of 5.75) is shown in Fig. 5 in which the donor (marked by number 1), donors wind (marked by number 2) and a disc (marked by number 3) are good seen. The cross-section of the calculation area by the $Z-Y$ plane lying on the accretor (the temperature contours and velocity field; the precession phase is about of 7.6) is shown in Fig. 6 (the low resolution space scale) and Fig. 7 (the high resolution space scale). In this figure the high temperature region in the vicinity of the disc centre is very good seen (marked by number 1). This region has the strong warped form.

The cross-sections of the calculation area by $Z-X$ plane on line of centres and the $Z-Y$ plane line on compact object centre on time of jet launch of 7.6 precession period are shown in Fig. 8 and Fig. 9. In Fig. 8 the donor-star is marked by number 1 and the L_1 stream is marked by number 2; in Fig. 9 the accretion disk is marked by number 1. As it is good seen from Fig. 8-9 the two-armed jets are launching on the time of 7.6 precession period.

4. Conclusions

To summarize the present simulations we may finally conclude that the essential numerical properties of both states, low/hard and high/soft, and jet production (the increasing of the disc central part temperature in low/hard state relatively high/soft; the decreasing of the disc mass accretion rate in low/hard state relatively high/soft; the transition between both states occurs at very short time scales it is the key property of the present simulations; the sudden jet production at the beginning of low/hard state; the maximal jet velocity occurs at the beginning and at the end of low/hard state) are close to the observed ones of classical microquasars.

References

Belotserkovskii O.M., Davydov Yu.M.: 1982, *The large particles code in gas dynamics, Moscow, Nauka,* 391.

Cox D. P., Daltabuit E.: 1971, *ApJ*, **167**, 113.

Fender R. et al.: 1999, *ApJ*, **519**, 165.

Fender R.: 2001, *MNRAS*, **322**, 31.

Fender R.P., Gallo E., Jonker P.: 2003, *MNRAS*, **343**, 99.

Fender R.P., Belloni T.M., Gallo E.: 2004, *MNRAS*, **355**, 1105.

Fender R. et al.: 2006, *MNRAS*, **369**, 603.

Gallo E., Fender R.P.: 2005, *MmSAI*, **76**, 600.

Gallo E.: 2007, *Ap&SS*, **311**, 161.

Lachowicz P. et al.: 2006, *MNRAS*, **368**, 1025.

Mirabel I.F.: 2001, *ApSSS*, **276**, 319.

Nazarenko V.V., Nazarenko S.V.: 2014, *Odessa Astron. Publ.*, **27**, 137.

Nazarenko V.V., Nazarenko S.V.: 2015, *Odessa Astron. Publ.*, **28**, 171.